TRANSPORT PROBLEMS 2018 Volume 13 Issue 1
PROBLEMY TRANSPORTU DOI: 10.21307/tp. 2018.13.1.12

Keywords: numerical simulation; non-linear dynamics; self-exciting vibration

Krzysztof ZBOINSKI*, Milena GOLOFIT-STAWINSKA
Warsaw University of Technology, Faculty of Transport
Koszykowa 75, 00-662 Warsaw, Poland
**Corresponding author*. E-mail: kzb@wt.pw.edu.pl

THE IMPACT OF PRIMARY SUSPENSION STIFFNESS OF 2-AXLE BOGIE OF MKIII PASSENGER CAR ON ITS DYNAMICAL BEHAVIOUR

Summary. This article presents results of the study on the impact of stiffness in vehicle primary suspension for lateral direction k_{zy} and longitudinal direction k_{zx}. The study was carried out for 2-axle bogie of MKIII passenger car. The problem was solved by numerical tests performed with the simulation software for dynamics of vehicle-track system. Performed study consisted in varying both stiffness types through change of their values from 0.001 to 1000 times as compared to nominal value.

1. INTRODUCTION

The question raised in this article is a part of the larger study involving identification of the parameters of the greatest impact, and study of this impact, on behaviour of the vehicle especially in the transition curve (TC) sections and near the non-linear critical velocity v_n. Non-linear critical velocity is not investigated by the authors in this article. Nevertheless the authors evaluated its values. The authors used approach applied in the earlier publications, e.g. [12]. This publication shows different values of v_n in straight track (ST) and circular curves (CC) and dependence of v_n on suspension stiffness parameters. As the non-linear critical velocity the authors understand minimum velocity at which vehicle hunting motion appears (in the model studies such motion is represented by the limit cycle being a stable periodic solution). The article takes account of the parameters whose significant impact is revealed by the publications on dynamics, including stability of vehicle motion in straight track and circular curves, e.g. [1-5, 8, 9 and 11-13]. Here studied parameters are the coefficients of stiffness in the vehicle primary suspension for lateral k_{zy} and longitudinal k_{zx} directions. The study was performed for 2-axle bogie of MKIII passenger car. The problem was solved by performing numerical tests using the simulation software built by the first author.

The results of a fairly extensive simulation study are presented in chapter 3. They were divided into four groups. First group represents the impact of the lateral stiffness k_{zy} on non-linear behaviour of the bogie. Stiffness value was lower than the basic value, i.e. the one for which results were obtained representing motivation to perform study. In the second group - just like in first one - studied was the influence of lateral stiffness k_{zy} on non-linear dynamics of the bogie. But this time the stiffness was greater than the nominal. In the third and fourth group studied was the impact of longitudinal stiffness k_{zx} on the non-linear behaviour of the object. As before - by analogy - in the third group longitudinal stiffness value is lower than the nominal, and in the fourth group is higher.

The next steps of the study will include the study of the impact of stiffness on non-linear behaviour of more complex vehicles such as rail cars. Analysis of the behaviour of 2-axis objects is easier, and makes an introduction to the study of 4-axle vehicles.

2. THE MODEL USED IN THE STUDY

The subject of the study in this article is a 2-axle bogie of MKIII passenger car. The nominal structure of this bogie model is shown in Fig. 1c. Bogie model was supplemented with discrete models of vertically and laterally flexible track, as shown in Figs. 1a and 1b. Parameters of the model are collected in tab. 1.

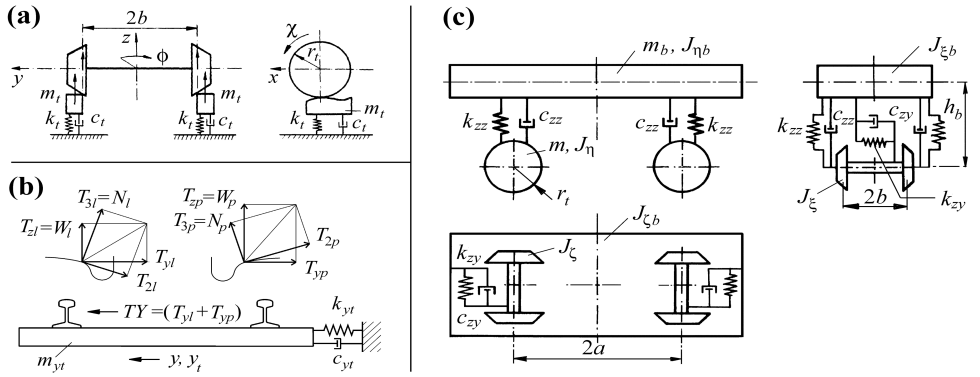

Fig. 1. Nominal models structure: a) track susceptible vertically, b) track susceptible laterally, c) the bogie [13]

Table 1

Parameters of the boogie of MKIII passenger car [14]

Notation	Parameter description	Measur. unit	Value of parameter
m_b	bogie frame mass	kg	2707
m	wheelset mass	kg	1375
$I_{\xi b}$	bogie frame moment of inertia; longitudinal axis	kg·m^2	1800
$I_{\eta b}$	bogie frame moment of inertia; lateral axis	kg·m^2	3500
$I_{\zeta b}$	bogie frame moment of inertia; vertical axis	kg·m^2	3500
I_{ξ}	wheelset moment of inertia; longitudinal axis	kg·m^2	790
I_{η}	wheelset moment of inertia; lateral axis	kg·m^2	100
I_{ζ}	wheelset moment of inertia; vertical axis	kg·m^2	790
k_{zz}	vertical stiffness of the 1st level of suspension	kN/m	880
k_{zy}	lateral stiffness of the 1st level of suspension	kN/m	1308
k_{zx}	longitudinal stiffness of the 1st level of suspension	kN/m	2667
c_{zz}	vertical damping of the 1st level of suspension	kNs/m	170
c_{zy}	lateral damping of the 1st level of suspension	kNs/m	0
c_{zx}	longitudinal damping of the 1st level of suspension	kNs/m	0
a	semi-wheel base	m	1,3
h_b	vertical distance between mass centres of wheelset and vehicle body	m	0,303
r_t	wheelset rolling radius	m	0,457
s_g	gravitational stiffness parameter.	-	0,038
m_t	vertical mass of the rail	kg	200
k_t	vertical stiffness of the rail	kN/m	70000
c_t	vertical damping of the rail	kNs/m	200
m_{ty}	lateral mass of the track	kg	500
k_{ty}	lateral stiffness of the track	kN/m	25000
c_{ty}	lateral damping of the track	kNs/m	500

The bogie – track model has 18 degrees of freedom. It utilizes Lagrange type II equations adapted to the description of relative motion. This model was also used in [13]. Principles of the model building are discussed e.g. in [14].

Description of the contact geometry is introduced into the model using the so-called contact parameters table generated by the ArgeCare RSGEO [7] program, and the forces using FASTSIM procedure [6].

In the course of the study the bogie was used fitted with a pair of wheel and rail profiles S1002 and UIC60, traveling on the track with standard European width in accordance with [10] 1435 mm, and rails inclination of 1:40. For object and track model linear characteristics of elastic and damping elements were assumed.

3. STUDY OF THE STIFFNESS INFLUENCE FOR 2-AXLE BOGIE OF MKIII PASSENGER CAR

The results presented in the article show the impact of the longitudinal k_{zx} and lateral k_{zy} stiffness of the primary suspension on non-linear behaviour of 2-axle bogie of MKIII passenger car for velocities above and below the critical value v_n. Symbols used in figures are as follows: y - lateral displacement and ψ - yaw angle. Indexes b, p and k represent bogie frame, front wheelset, and rear wheelset respectively. Index o is used for "original" courses the, i.e. those which constituted motivation for the study. In the case of studied object the "original" graph was obtained for v=54 m/s, k_{zy}=1308000 N/m, k_{zx}=2667000 N/m and R=600 m. In addition the following designations are used: /0.1x, /4x, /20x, /100x to scale the stiffness and /10, /20, /30, /32, /33, /34, /36, /38, /39, /40, /42, /44, /45, /46, /48, /50, /54, /60, /62, /63, /65, /75 and /90 for velocitiess in m/s.

Simulations were performed for the object moving always along the route consisting of three consecutive sections: straight track, transition curve and circular curve. Individual sections of the route were designated on figures as follows: straight track - ST, transition curve – TC, and circular curve - CC. The lengths of the individual sections are as follows: straight track – 100 m, transition curve – 140 m, circular curve 100 m. Few simulations for long stretches of the route were made. Transition curve is always a parable of 3rd degree. Superelevation h was always selected in a way to balance components of the forces of gravity and centrifugal force in plane of the track. Maximum superelevation value permitted in Poland i.e. h = 150 mm was assummed. Initial transverse displacement $y_i(0)$=0.0045 m was imposed for all cases. Studies for a broad range of stiffness values were carried out:

- lateral k_{zy} – 0.001; 0.01; 0.1; 0.2; 0.4; 0.6; 0.8; 0.9; 2; 3; 4; 5; 6; 7; 8; 10; 100 and 1000 times compared to the nominal value,
- longitidunal k_{zx} – 0.001; 0.01; 0.1; 0.2; 0.4; 0.6; 0.7; 0.8; 0.9; 10; 20; 40; 60; 80; 90; 100 and 1000 times compared to the nominal value,

and a wide range of velocities from v=5 m/s until the numerical derailment.

Only the most representative figures were selected for the article. However the proposals concern the whole study group.

Values of lateral k_{zy} and longitudinal k_{zx} stiffness variants of suspension system, and vehicle velocity are given in captions under the figures.

3.1. Results for primary suspension lateral stiffness k_{zy} variants – the k_{zy} lower than nominal

Study results provided in this section were made with lateral stiffness k_{zy} and velocity v variants. Variants for lateral stiffness were prepared in the range of 0.001 to 0.9 times the nominal value k_{zy}=1308000 N/m, and amounted to k_{zy}=1308, 13080, 130800, 261600, 523200, 784800, 1046400 and 1177200 N/m. Variants were also prepared for vehicle velocity in the range of v=5 m/s to v=54 m/s. Fig. 2 shows lateral displacements of the front wheelset for: the case constituting motivation; the stiffness k_{zy}=130800 N/m (0.1x) and v=54 m/s; and stiffness k_{zy}=1177200 N/m (0,9x) and different

velocities. For the 10 times lower stiffness, oscillation amplitudes in ST, and TC are slightly higher than for the "original" chart but the object in the TC derails. Therefore simulations were performed for the stiffness ranging from 0.1 to 0.9 times the nominal value. The same figure contains waveforms obtained for the stiffness k_{zy}= 1177200 N/m (0.9x) and velocities of v=54, 50, 40, 39, 30, and 10 m/s. Charts obtained for v=54 m/s and stiffness 0.9x are similar to the "original" graph. Graphs obtained for slightly lower velocity of v=50 m/s are similar to the "original" but have a smaller amplitude. In both cases oscillations in ST increase, and in CC limit cycle is fixed but with very small amplitudes. For velocity of v=40 m/s oscillations at the end of the TC decrease, to later increase slightly in CC. While for the velocity lower by 1 m/s, i.e. v=39 m/s from the beginning of the route oscillations decrease, and by the end of TC die out, and doesn't excite again. There are no oscillations in CC. For lower velocities there are no oscillations in TC and CC.

Fig. 3 shows two curves of lateral displacements of the front wheelset obtained for v=50, and 54 m /s, and stiffness k_{zy}= 784800 N/m (0.6x). For higher velocities higher amplitude in ST, and TC were obtained. Oscillations in the TC die out while in CC they stabilize setting the limit cycle with low amplitude. While for lower velocities oscillations decrease to the end. No limit cycle in CC appears.

Fig. 4 shows graphs obtained for the stiffness as in Fig. 3 but for the velocity of v=50, 46, 44, 40, 30. For velocity of 50 and 46 m/s oscillations in ST increase. For velocities below 44 m/s they decrease. Which proves that the critical velocity in ST exists for velocities between v=44 m/s and v=46 m/s. For velocities of 46, 44, and 40 m /s limit cycle is fixed in CC. For velocity of 30, and 10 m/s there is no limit cycle in CC.

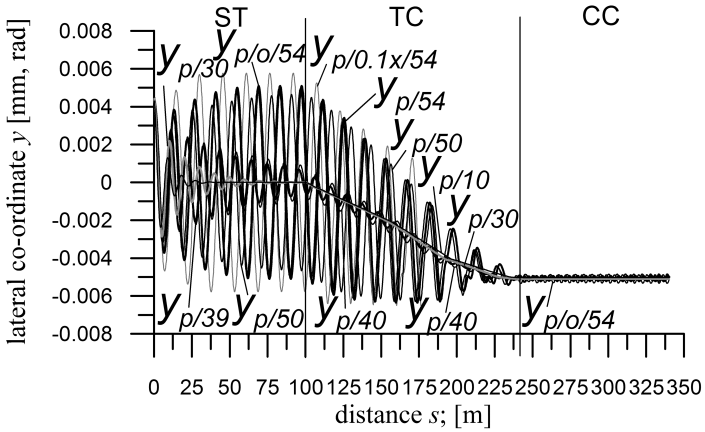

Fig. 2. Leading wheelset lateral displacements of 2-axle bogie of MKIII passenger car: non-zero initial conditions $y_i(0)$=0,0045 m, R=600 m, h=0,150 m, k_{zy}=1177200 N/m, v – different velocities

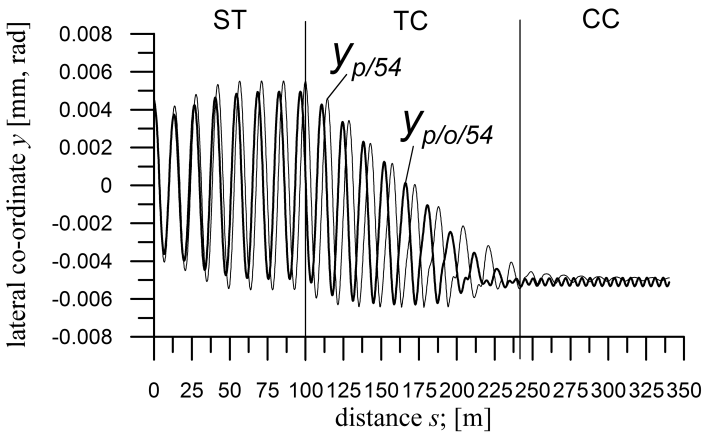

Fig. 3. Leading wheelset lateral displacements of 2-axle bogie of MKIII passenger car: non-zero initial conditions $y_i(0)$=0,0045 m, R=600 m, h=0,150 m, k_{zy}=784800 N/m, v=54 m/s

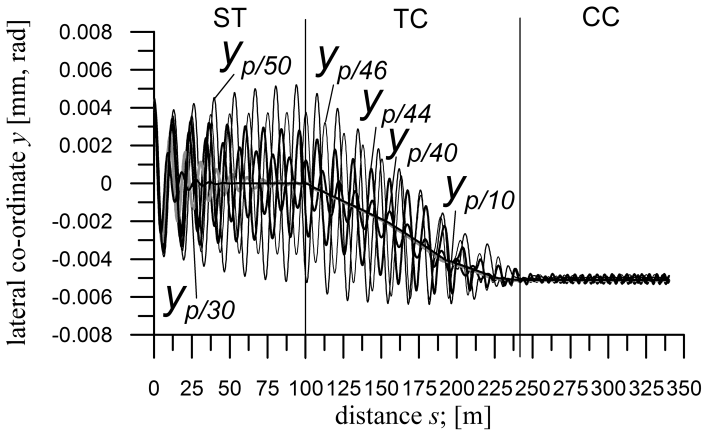

Fig. 4. Leading wheelset lateral displacements of 2-axle bogie of MKIII passenger car: non-zero initial conditions $y_i(0)$=0,0045 m, R=600 m, h=0,150 m, k_{zy}=784800 N/m, v – different velocities

3.2. Results for primary suspension lateral stiffness k_{zy} variants – the k_{zy} higher than nominal

Study results provided in this section were made with lateral stiffness k_{zy} and velocity v variants. Variants for lateral stiffness were prepared in the range of 2 to 1000 times the nominal value k_{zy}=1308000 N/m and amounted to k_{zy}=2616000, 3924000, 5232000, 6540000, 7848000, 9156000, 10464000, 11772000, 13080000, 130800000, and 1308000000 N/m. Variants were also prepared for vehicle velocity in the range from v=40 m/s to numerical derailment.

Fig. 5 shows the lateral displacements, and yaw angles of the front wheelset obtained by numerical simulation for the stiffness k_{zy}=5232000 N/m (4x), and velocity v=54 m/s and graph constituting motivation to take up the study. For an object of greater stiffness lower amplitude of oscillations was recorded in the ST, and TC while in CC limit cycle was obtained but with a greater amplitude than the limit cycle in CC in "original" graph. In both cases oscillations at the end of TC die out, just to re-excite in CC.

The graphs in Figs. 6 and 7 were obtained for the same stiffness (as previously) (k_{zy}=5232000 N/m), but Fig. 6 was made for velocities higher than v=54 m/s, and Fig. 7 for velocities lower than v=54 m/s.

Fig. 6 shows the lateral displacement and yaw angles for a front wheelset obtained for the velocities of v=54, 60, 65, 75, and 90 m/s. Graph obtained for the velocity of v=60 m/s has similar waveform to that obtained for the velocity of v=54 m/s. Oscillations on the graph for the velocity of v=65 m/s die out in the middle of TC and then re-excite, and at the end of TC die out again (creating a "bubble"), and setting a limit cycle in CC but with a very small amplitude. Graph obtained for the velocity of v=75 m/s is similar to the previous one, with such change in oscillations that at the end of TC they die out completely, and do not occur in CC. For velocity of v=90 m/s oscillations are stretched and die out in TC. In CC there are also no oscillations. In all cases in ST the limit cycle was observed.

Fig. 7 also shows the lateral displacements and yaw angles for the front wheelset obtained for the same stiffness as before but for velocities of v=40, 45, 50, and 54 m/s. In addition, for the velocity below v=54 m/s the last section of the route was extended to 300 m. Waveforms for the velocity of v=50 m/s are similar to those obtained for the velocity of v=54 m/s. The difference lies only in the fact that oscillations in CC excite a little later. Limit cycle is fixed. For the velocity of v=45 m/s there is no limit cycle in ST. Oscillations steadily decrease right from the start. In TC no oscillation appears. In CC oscillations re-appear, limit cycle is fixed but with small amplitude. For the velocity of v=40 m/s no oscillations in TC, and CC exist.

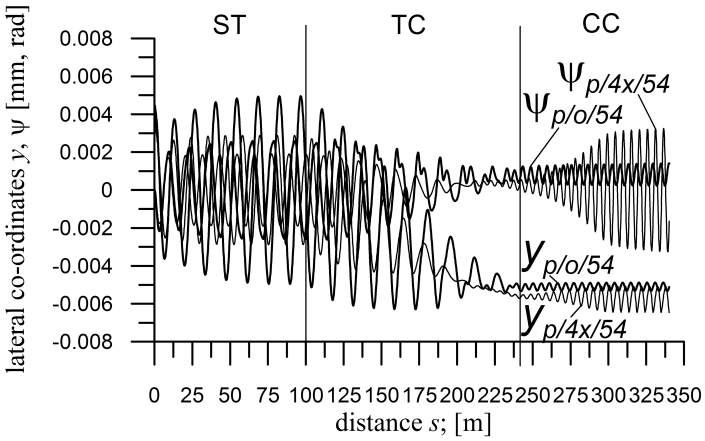

Fig. 5. Selected co-ordinates of 2-axle bogie of MKIII passenger car: non-zero initial conditions $y_i(0)$=0,0045 m, R=600 m, h=0,150 m, k_{zy}=5232000 N/m, v= 54 m/s

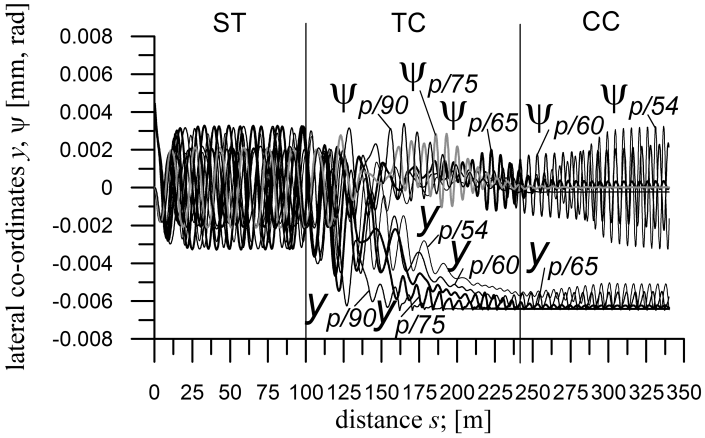

Fig. 6. Selected co-ordinates of 2-axle bogie of MKIII passenger car: non-zero initial conditions $y_i(0)$=0,0045 m, R=600 m, h=0,150 m, k_{zy}=5232000 N/m, v – different velocities

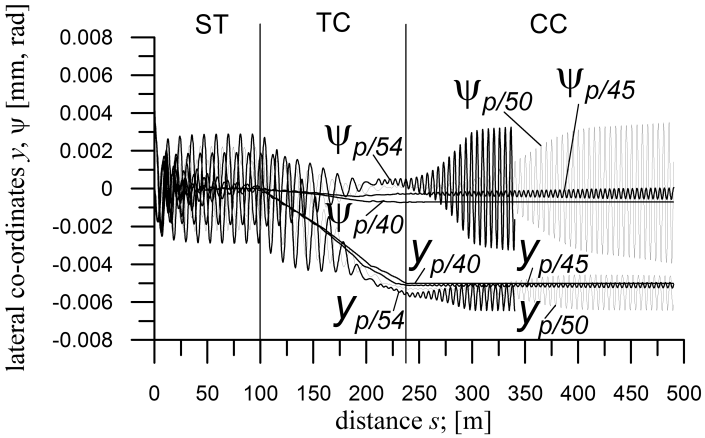

Fig. 7. Selected co-ordinates of 2-axle bogie of MKIII passenger car: non-zero initial conditions $y_i(0)$=0,0045 m, R=600 m, h=0,150 m, k_{zy}=5232000 N/m, v – different velocities

3.3. Results of primary suspension longitudinal stiffness k_{zx} variants – the k_{zx} lower than nominal

Study results provided in this section were made with longitudinal stiffness k_{zx} and velocity v variants. Variants for longitudinal stiffness were prepared in the range of 0.001 to 0.9 times the nominal value k_{zy}=2667000 N/m, and amounted to k_{zy}=2667, 26670, 266700, 2400300, 2133600, 1866900, 1600200, 1333500, 1066800, 800100, 533400 and 266700 N/m. Variants were also prepared for vehicle velocity in the range of v=5 m/s to v=54 m/s.

Fig. 8 shows lateral displacements of the front wheelset for: the example constituting motivation (stiffness k_{zx}=266700 N/m, velocity v=54 m/s); and stiffness k_{zx}=1600200 N/m (0.6x) and different velocities. For the velocity of v=54 m/s but reduced stiffness oscillations steadily decrease in TC and CC. In CC they die out at the end. For the velocity of v=50 m/s oscillations die out a little earlier, and do not occur in CC. For both velocities the occurrence of limit cycle in ST was recorded. For the velocity of v=40 m/s oscillations pass smoothly from ST through TC reaching the limit cycle in CC. For the velocity of v=30 m/s and lower, oscillations in ST tend to decrease. They do not occur in TC, and CC. For small velocities oscillations in CC do not occur. For the velocity of v=40 m/s limit cycle occurs in CC. For small velocities v=50 m/s oscillations in CC do not occur. For small velocities v=54 m/s oscillations in CC do occur but have the tendency to die out.

Fig. 9 shows waveforms for a range of velocities starting from v=40 m/s to v=50 m/s and longitudinal stiffness k_{zx}=1600200 N/m (0.6x). For all the velocities from the above range the limit cycle was obtained in ST. Oscillations pass smoothly into TC. In CC for v=50 m/s there are no oscillations. For the velocities of v=48 and 46 m/s oscillations are small and die out. For velocities of v=44, 42, and 40 m/s limit cycle is fixed.

Fig. 10 shows the lateral displacements of the front wheelset for the velocity range of v=30 m/s to v=40 m/s and longitudinal stiffness k_{zx}=1600200 N/m (0.6x). For the velocity of v=40 m/s oscillation amplitude in ST increase, and then smoothly decrease in the TC. In circular curve limit cycle is fixed at small amplitude. For the velocity of v=39 m/s over entire length of the ST oscillation amplitude reaches similar values, in TC increases and in CC decreases, and limit cycle is fixed. For the velocity of v=38 m/s limit cycle in ST was not reached, which indicates the existence of a critical velocity in ST between 38 and 39 m/s. In ST, and TC smaller oscillation amplitude was recorded relative to the amplitudes obtained at the higher velocities. In CC limit cycle occurs. For the velocity of v=36 m/s oscillation amplitudes decrease over the entire length of the route. In CC oscillations die out. For the velocity of v=30 m/s no oscillations in TC, and CC.

Fig. 11 shows all the co-ordinates for longitudinal stiffness k_{zx}=1600200 N/m (0.6x), and velocity of v=39 m/s. In all cases oscillation amplitudes in TC increase in relation to the amplitude in ST and then decrease smoothly passing into CC. In CC in all cases limit cycle is fixed but with small amplitudes.

Figs. 12 to 15 were made for the stiffness k_{zx}=1066800 N/m (0.4x) and a wide velocity range. The fig. 12 shows the lateral displacements of the front and rear wheelset for the velocities of v=40, 30, 20, and 10 m/s and the rear wheelset displacement for the case constituting motivation (k_{zx}=2667000 N/m, and v=54 m/s). For the velocity of v=40 m/s object derails in ST. For the velocity of v=30 m/s (velocity below the critical one in ST) oscillations smoothly drop down in ST, in TC they almost die out, and at the beginning of the CC they die out completely. For smaller velocities oscillations die out already in ST. They do not occur in TC and CC.

Fig. 13 shows waveforms in the range from v=30 to v=40 m/s for the rear wheelset. For v=40, 38, and 36 m/s object derails at the very beginning of its route (in the initial section of ST). For v=34 m/s it happens at the end of ST section. For v=33 m/s oscillations smoothly pass from ST through TC into CC. At the end of TC oscillations tend to increase, and in CC limit cycle with large amplitude is fixed. For v=32 m/s oscillations tend to decrease right from the beginning. In CC they die out completely. Graphs for two velocities v=33 and 32 m/s show, that the critical velocity in the ST is for the velocity lying between these two. For v=30 m/s oscillations also tend to decrease right from the start. At the end of TC they die out. Oscillations do not occur in CC.

Fig. 14 shows the lateral co-ordinates for longitudinal stiffness value as before and the velocity of v=33 m/s. For the front wheelset oscillations smoothly pass from ST to CC. Oscillation amplitude

along the entire route is similar. In CC along entire length there is a limit cycle. For the final wheelset oscillations also pass smoothly through the various sections of the route but tend to increase. In CC limit cycle is fixed with a relatively large amplitude. For bogie frame lateral displacements pass smoothly from ST, through TC, into CC creating limit cycle in CC, whereas yaw angles ψ tend to increase, and lower oscillation amplitude over the whole route length compared to other co-ordinates.

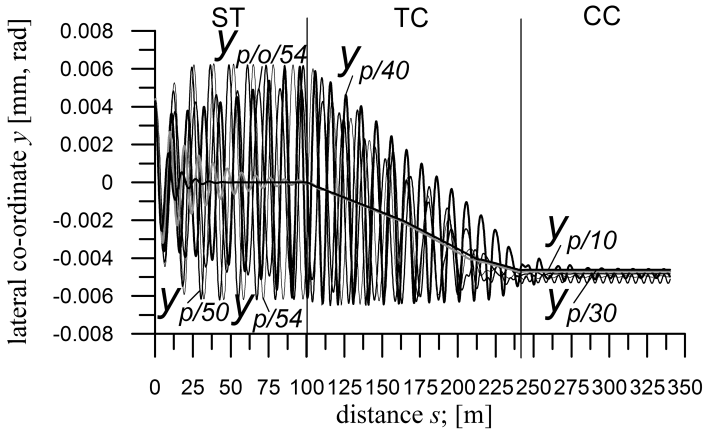

Fig. 8. Leading wheelset lateral displacements of 2-axle bogie of MKIII passenger car: non-zero initial conditions $y_i(0)$=0,0045 m, R=600 m, h=0,150 m, k_{zx}=1600200 N/m, v – different velocities

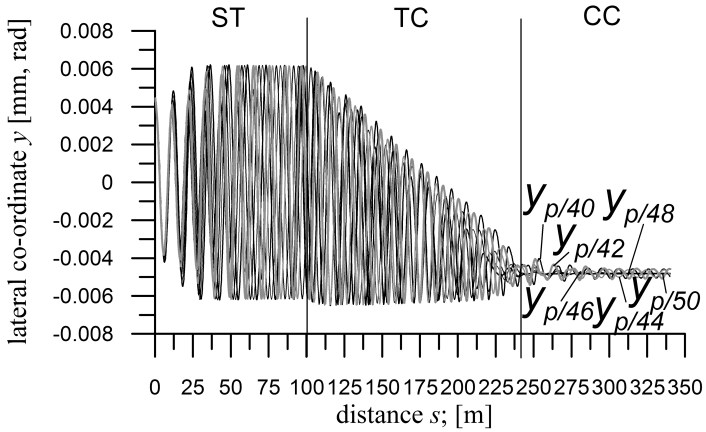

Fig. 9. Leading wheelset lateral displacements of 2-axle bogie of MKIII passenger car: non-zero initial conditions $y_i(0)$=0,0045 m, R=600 m, h=0,150 m, k_{zx}=1600200 N/m, v – different velocities

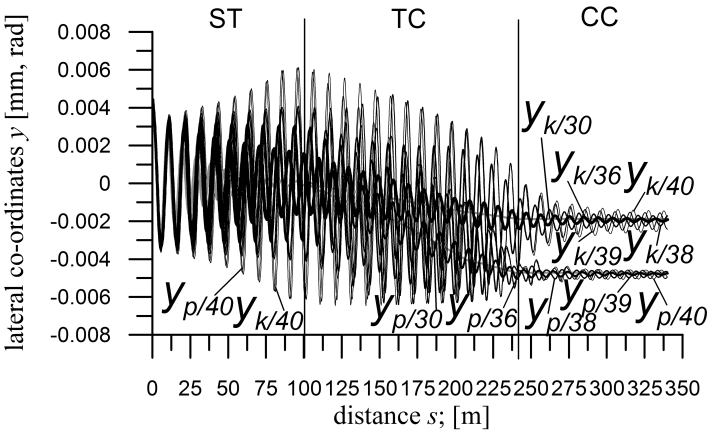

Fig. 10. Selected co-ordinates of 2-axle bogie of MKIII passenger carriage: nonzero initial conditions $y_i(0)$=0,0045 m, R=600 m, h=0,150 m, k_{zx}=1600200 N/m, v – different velocities

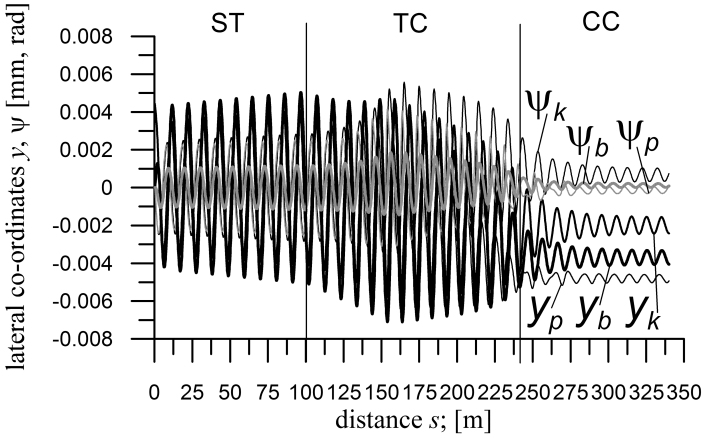

Fig. 11. Selected co-ordinates of 2-axle bogie of MKIII passenger car: non-zero initial conditions $y_i(0)$= 0,0045 m, R=600 m, h=0,150 m, k_{zx}=1600200 N/m, v=39 m/s

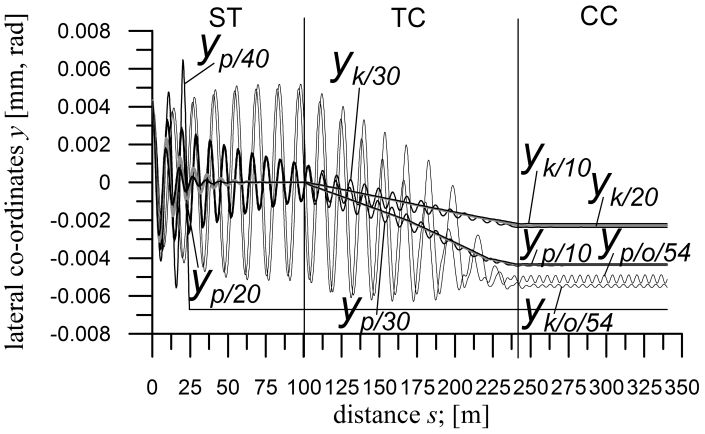

Fig. 12. Selected co-ordinates of 2-axle bogie of MKIII passenger car: non-zero initial conditions $y_i(0)$= 0,0045 m, R=600 m, h=0,150 m, k_{zx}=1066800 N/m, v – different velocities

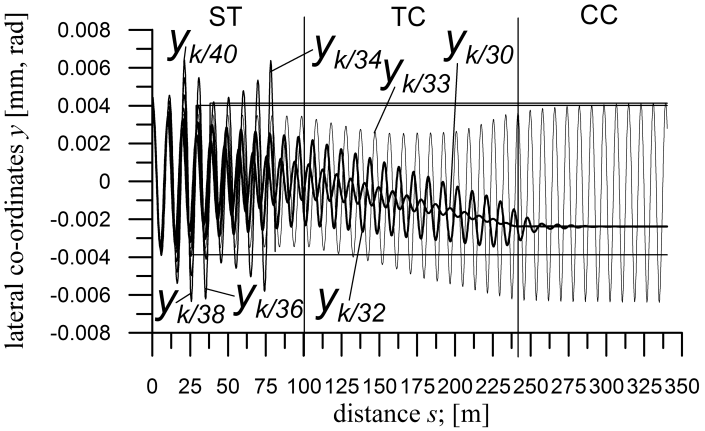

Fig. 13. Rear wheelset lateral displacements of 2-axle bogie of MKIII passenger car: non-zero initial conditions $y_i(0)$=0,0045 m, R=600 m, h=0,150 m, k_{zx}=1066800 N/m, v – different velocities

Fig. 15 shows all of the co-ordinates for longitudinal stiffness as before and the velocity of v=32 m/s (1 m/s lower than in Fig. 14). For all co-ordinates oscillations over the entire length of the route tend to decrease, and in CC they die out.

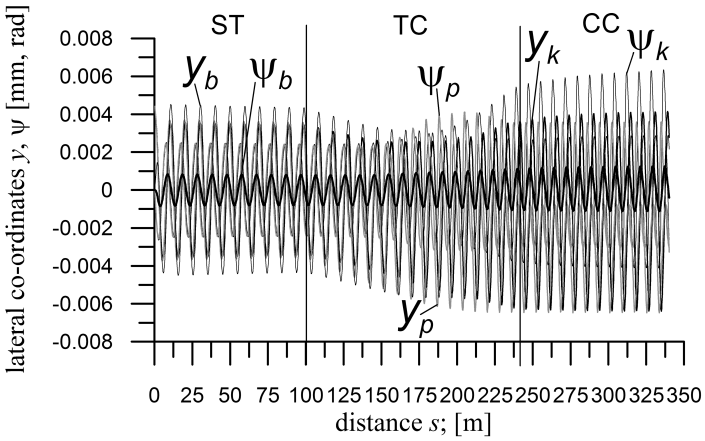

Fig. 14. Selected co-ordinates of 2-axle bogie of MKIII passenger car: non-zero initial conditions $y_i(0)$= 0,0045 m, R=600 m, h=0,150 m, k_{zx}=1066800 N/m, v=33 m/s

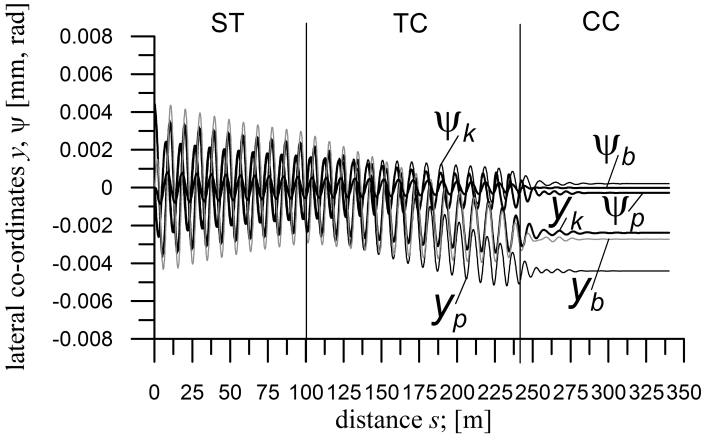

Fig. 15. Selected co-ordinates of 2-axle bogie of MKIII passenger car: non-zero initial conditions $y_i(0)$= 0,0045 m, R=600 m, h=0,150 m, k_{zx}=1066800 N/m, v=32 m/s

3.4. Results for primary suspension longitudinal stiffness k_{zx} variants – the k_{zx} higher than nominal

Study results provided in this section were made with longitudinal stiffness k_{zx} and velocity v variants. Variants for longitudinal stiffness were prepared in the range of 10 to 1000 times the nominal value k_{zy}=2667000 N/m, and amounted to k_{zy}=26670000, 53340000, 106680000, 160020000, 213360000, 240030000, 266700000 and 2667000000 N/m. Variants were also prepared for vehicle velocity in the range of v=54 m/s to v=70 m/s.

Fig. 16 shows the lateral displacements and rotation angles of the front wheelset for the velocity of v=54 m/s and nominal longitudinal stiffness („original" graph), k_{zx}=26670000 N/m (10x), k_{zx}=53340000 N/m (20x) and k_{zx}=266700000 N/m (100x). Limit cycle in CC was obtained only for the "original" graph. In other cases oscillations at the end of TC die out. Also for the "original" graph oscillations in ST achieve the greatest oscillation amplitude.

Fig. 17 was made for the stiffness k_{zx}=53340000 N/m (20x), and velocities in the range of v=54 m/s to v=70 m/s. With the increase in velocity the oscillation amplitude increases in ST and CC. In all cases oscillations tend to die out, and die out at the end TC. Oscillations do not occur in CC. For the velocity of v=63 m/s bogie derails in TC.

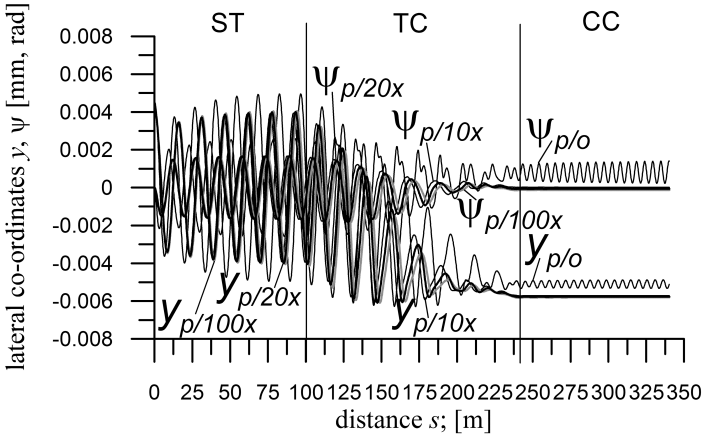

Fig. 16. Selected co-ordinates of 2-axle bogie of MKIII passenger car: non-zero initial conditions $y_i(0)$= 0,0045 m, R=600 m, h=0,150 m, k_{zx} – different stiffness, v=54 m/s

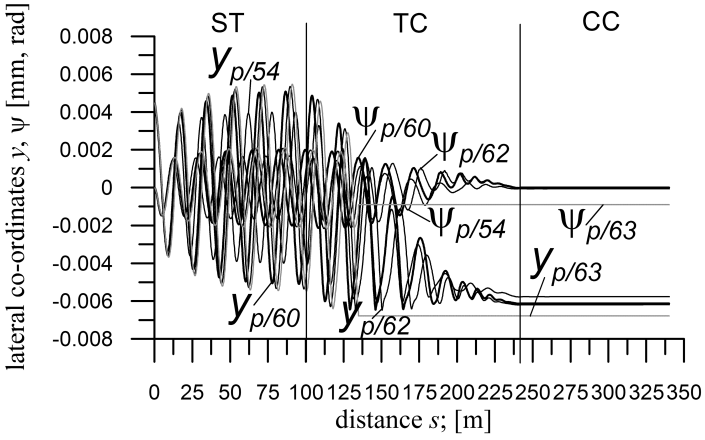

Fig. 17. Selected co-ordinates of 2-axle bogie of MKIII passenger car: non-zero initial conditions $y_i(0)$= 0,0045 m, R=600 m, h=0,150 m, k_{zx}=53340000 N/m, v – different velocities

4. CONCLUSIONS

Studies of the impact of lateral k_{zy} and longitudinal k_{zx} stiffness on non-linear behaviour of 2-axle bogie of MKIII passenger car showed a multitude of solutions both in TC and CC. Along with the successive results more questions appeared. Some results require further investigation and explanation of the causes of occurrence or non-occurrence of the oscillations.

Lateral stiffness k_{zy} can be raised several times in relation to the nominal value. However, when reducing the lateral stiffness k_{zy} object quickly derails. Fairly high critical velocity v_n in ST and CC was achieved. Reducing lateral stiffness k_{zy} and velocity v causes decrease in amplitude of limit cycles or their disappearance in CC. Increase in lateral stiffness k_{zy} and the velocity v also causes reduction in amplitude of limit cycles in CC or disappearance of oscillations in CC. The increase in lateral stiffness k_{zy} in relation to the nominal value for the velocity v=54 m/s (graph that constitutes motivation to study) results in a reduction in the oscillation amplitude in ST, and TC while in CC limit cycle was obtained but with amplitude greater than for the nominal stiffness.

As in the case of lateral stiffness k_{zy} also longitudinal stiffness k_{zx} can be raised several times in relation to the nominal value. However, when reducing the longitudinal stiffness k_{zx} the object quickly derails. For the nominal velocity of v=54 m/s but reduced longitudinal stiffness oscillations on the route decrease and at the end of CC die out. For small velocities and reduced longitudinal stiffness oscillation amplitudes decrease or oscillations die out, and in CC do not occur. For the smallest

longitudinal stiffness and velocity of v=33 m/s oscillations smoothly pass from ST trough TC, and in CC limit cycle was obtained with large amplitude. For the high longitudinal stiffness - in all cases – the oscillations already at the end of TC die out, and do not occur in CC.

ACKNOWLEDGEMENTS

Scientific work carried out as research project no. 2014/15/N/ST8/02668 from funds of National Science Centre, Poland.

References

1. Abood, K.H.A. Khan, R.A. Influence of vertical primary suspension stiffness parameter on dynamic response of railway bogie. *International Review of Mechanical Engineering*. 2011. Vol. 5(1). P. 173-179.
2. Cheng, Y.C. & Lee, S.Y. & Chen, H.H. Modelling and nonlinear hunting stability analysis of high-speed railway vehicle on curved tracks. *Journal of Sound and Vibration*. 2009. Vol. 324. No. 1-2. P. 139-160.
3. Droździel, J. & Sowiński, B. Railway car dynamic response to track transition curve and single standard turnou*t*. In: Allan, J. (ed. et al.). *Computers in Railway X. Computer System Design and Operation in the Railway and other transit systems.* WIT Press. 2006. P. 849-858.
4. Hoffmann, M. *Dynamics of European two-axle freight wagons*. PhD thesis. Technical University of Denmark. Informatics and Mathematical Modelling. Lyngby. Denmark. 2006. 159 p.
5. Hoffmann, M. & True, H. The dynamics of European two-axle railway freight wagons with UIC standard suspension. *Vehicle System Dynamics*. 2008. Vol. 46. No. Suppl. P. 225-236.
6. Kalker, J.J. A fast algorithm for the simplified theory of rolling contact. *Vehicle System Dynamics.* 1982. Vol. 11. P. 1-13.
7. Kik, W. Comparison of the behaviour of different wheelset-track models. *Vehicle System Dynamics*. 1992. Vol. 20. No. Suppl. P. 325-339.
8. Mohan, A. & Ahmadian, M. Nonlinear investigation of the effect of suspension parameters on the hunting stability of a railway truck. *Proceedings of the 2006 IEEE/ASME Joint Rail Conference*. 4-6 April 2006. P. 327-336. DOI: 10.1109/RRCON.2006.215325.
9. Polach, O. Characteristic Parameters of Nonlinear Wheel/Rail Contact Geometry. *Vehicle System Dynamics*. 2010. Vol. 48. No. Suppl. P. 19-36.
10. Sysak, J. (red.). *Drogi kolejowe*. Polskie Wydawnictwo Naukowe. Warszawa. 1986. 962 p. [In Polish: Sysak, J. (ed.). Railway roads. Polish Scientific Publishers. Warsaw].
11. Wang, K. & Liu, P. Lateral stability Analysis of Heavy-Haul Vehicle on Curved Track Based on Wheel/Rail Coupled Dynamics. *Journal of Transportation Technologies*. 2012. Vol. 2. P. 150-157.
12. Zboinski, K. & Dusza, M. Bifurcation analysis of 4-axle rail vehicle models in a curved track. *Nonliniear Dynamics*. 2017. Vol. 89(2). P. 863-885. DOI: 10.1007/s11071-017-3489-y.
13. Zboinski, K. & Golofit-Stawinska, M. Dynamics of 2 and 4-Axle Railway Vehicles in Transition Curves above Critical Velocity. In: Pombo J. (ed.). *Proceedings of the Second International Conference on "Railway Technology: Research, Development and Maintenance"*. Stirlingshire, UK. Civil-Comp Press. Paper 265. 2014. DOI:10.4203/ccp.104.265.
14. Zboinski, K. Importance of imaginary forces and kinematic type non-linearities for description of railway vehicle dynamics. *Proc. IMechE Part F Journal of Rail and Rapid Transit*. 1999. Vol. 213(3). P. 199-210.

Received 31.01.2017; accepted in revised form 15.03.2018